

LRP 595/98

January 1998

TOROIDALLY ASYMMETRIC ELM  
PRECURSORS IN TCV

H. Reimerdes, A. Pochelon  
& W. Suttrop

accepted for publication in  
Nuclear Fusion

21

# Toroidally Asymmetric ELM Precursors in TCV

H. Reimerdes, A. Pochelon, W. Suttrop†

Centre de Recherches en Physique des Plasmas,  
Association EURATOM – Confédération Suisse,  
Ecole Polytechnique Fédérale de Lausanne,  
1015 Lausanne, Switzerland

†Max-Planck Institut für Plasmaphysik,  
IPP – EURATOM Association, 85748 Garching, Germany

## Abstract

Coherent magnetic oscillations precede ELMs in TCV. The precursor has been detected prior to ELMs considered to be of type III and others previously referred to as TCV large ELMs. This permits the identification of both as type III ELMs according to the usual classification scheme. The strong localization of these precursors on the bad curvature side of the plasma and their medium toroidal mode numbers indicate their ballooning character. Unlike conventional MHD modes, these modes start toroidally localized and grow in amplitude and toroidal extent. When the precursor encompasses the whole toroidal circumference, the increased transport phase, as indicated by the characteristic  $D_\alpha$  spike, begins.

## 1 Introduction

In TCV ( $R = 0.89$  m,  $a = 0.25$  m,  $I_P < 1.2$  MA,  $B_\phi < 1.5$  T) quasi-stationary ohmic H-modes have been obtained in the presence of ELMs. The observed ELM spectrum is continuous and ranges from ELMs considered to be of type III to low frequency ELMs referred to as large ELMs [1]. An unambiguous classification in the usual scheme [2], for example by performing a scan of auxiliary heating power, has so far not been possible.

Prior to both types of ELMs, coherent magnetic oscillations, indicating a rapidly growing MHD instability, have been observed. The structure of these precursor oscillations is investigated with Mirnov probe arrays, which are installed inside the vacuum vessel and measure the poloidal magnetic field  $B_\theta$ . The first cutoff frequency of the pick-up coils is at 130 kHz and data is sampled up to a rate of 1 MHz.

## 2 Magnetic ELM precursors

### 2.1 Toroidal measurements

For high- $n$  mode analysis there are two complete toroidal arrays of 16 and 8 equally spaced probes, located on the equatorial low field side (LFS) and high field side (HFS) respectively. To maximize the signal amplitude, in spite of multipole field decay, the distance between plasma and magnetic probes was minimized, yielding a minimum distance of 5 cm between the separatrix and the toroidal probe array on the HFS and 7.5 cm on the LFS.

The ELMs obtained in these discharges have caused a moderate particle loss of 2-4% and an energy loss of 2-6% of the total plasma content, which are typical figures for type III ELMs in TCV. Their repetition frequency ranges from 120 to 300 Hz.

For many ELMs a coherent precursor oscillation has been detected several 100  $\mu$ s before the onset of the enhanced particle transport phase corresponding to the rise of the  $D_\alpha$ -signal. The precursor is only detected on the LFS (see Fig. 1), even though the distance between probes and plasma is greater than on the HFS.

The ELM precursor first develops at a toroidally localized position (Fig. 2b), A). This instability then grows both in amplitude and toroidal extent with a typical growth time of

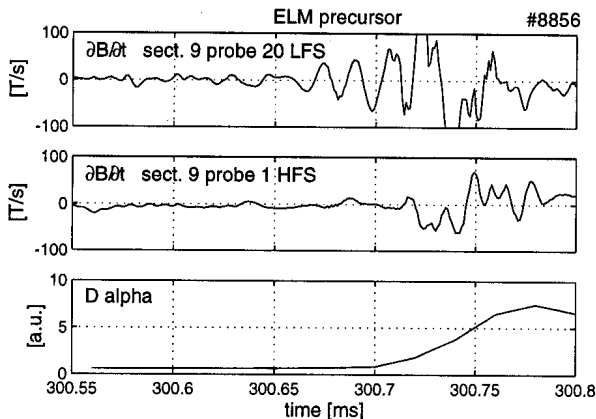


Figure 1:  $\partial B_\theta/\partial t$  measured on the LFS and HFS. The ELM precursor is only detected on the LFS even though the distance there between separatrix and probe is greater.

$\tau_{\text{prec}} = 50 \mu\text{s}$  (Fig. 2b), B). At the same time the frequency  $f_{\text{prec}}$  decreases from typically 120 to 70 kHz. The position of the instability rotates toroidally in the electron diamagnetic drift direction. When the precursor encompasses the whole toroidal circumference the increased transport of energy and particles, as indicated by the increase of the  $D_\alpha$  signal, begins. The magnetic oscillations lose their coherence while the fluctuation amplitude rises strongly (Fig. 2b), C). Due to the rotation of the toroidally localized precursor, measurements taken at one toroidal location show apparent characteristics of beating as have been observed on other experiments [3, 4].

The toroidal position of the onset of the precursor differs from ELM to ELM. Occasionally a simultaneous onset of the precursor at two toroidal positions is observed. The two positions are always toroidally  $180^\circ$  apart and also rotate in the electron diamagnetic drift direction.

## 2.2 Toroidal mode spectrum

The spatial measurements of magnetic fluctuations  $B_\theta$  on the LFS at toroidal positions  $\phi_k$  ( $k = 1, \dots, 16$ ) have been decomposed into Fourier coefficients

$$c_n(t) = \frac{1}{8} \sum_{k=1}^{16} B_\theta(\phi_k, t) \exp(in\phi_k) \quad (1)$$

yielding amplitudes  $A_n = \|c_n\|$  of toroidal mode components with mode numbers of  $n = 0, 1, \dots, 8$ . The precursor consists of medium  $n = 6 - 8$ , predominantly 7 and 8, components (Fig. 3), but spatial aliasing could possibly mask higher mode numbers such as 9 or 10. The  $n = 6 - 8$  components grow with a typical growth time of  $50 \mu\text{s}$ , whereas the

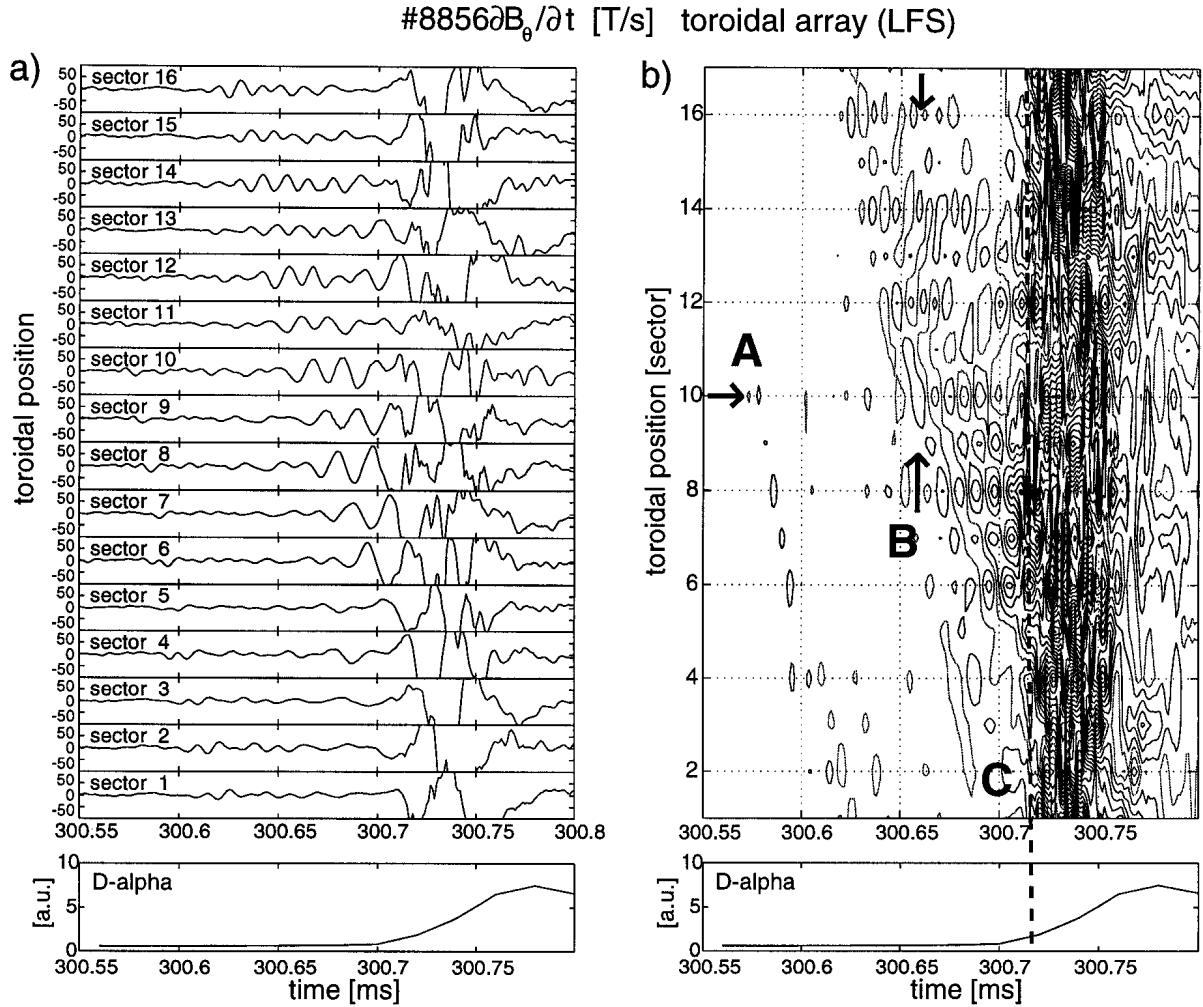


Figure 2: a) Measurements of  $\partial B_\theta / \partial t$  with the toroidal array on the LFS show coherent ELM precursor oscillations. The  $D_\alpha$  signal indicates the onset of the enhanced radial transport phase.

b) Contour lines of the same measurements show the toroidally localized onset (A) of the precursor. The precursor grows in amplitude and toroidal extent (B). When it encompasses the whole toroidal circumference the increased transport phase begins (C).

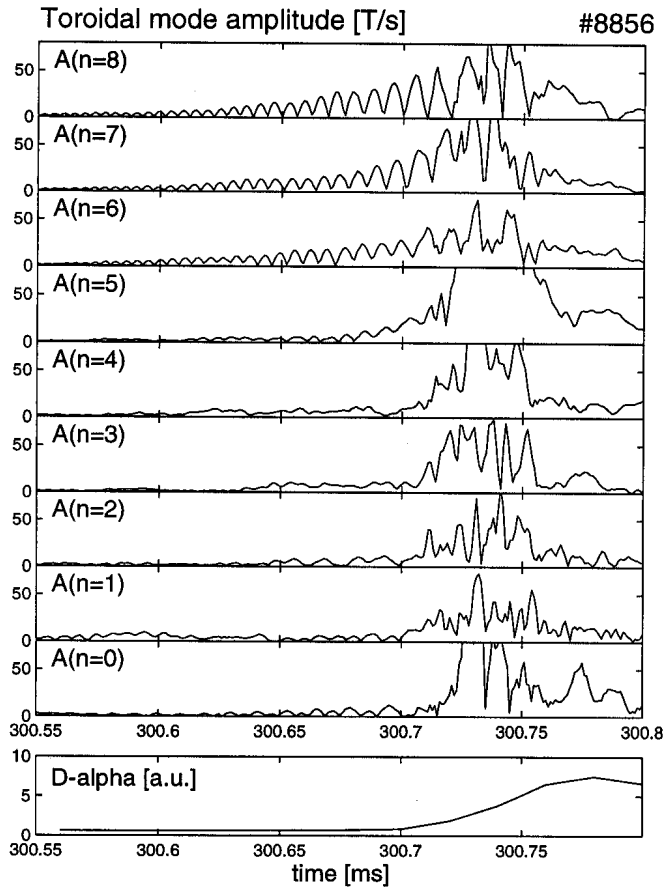


Figure 3: Toroidal mode amplitudes of the ELM precursor of Fig. 2, deduced from the 16 equally spaced probes on the LFS. The amplitude of the  $n = 5 - 8$  components grow over several  $100 \mu\text{s}$ . The beginning of the enhanced transport phase indicated by the increase of the  $D_\alpha$  signal is accompanied by a broadening of the mode spectrum.

lower components start to grow only immediately before the enhanced transport phase. The toroidal phase velocity increases with increasing mode number.

The amplitude of the  $n = 8$  signal shows an oscillation with twice the precursor frequency. Since the  $n = 8$  is the spatial correspondence  $n_{Ny}$  of the Nyquist frequency the zeros in its amplitude are caused by the passing of the zeros of  $\sin(8\phi)$  by the position of the probes. However, oscillations are also observed on lower  $n$  mode amplitudes. They have the same frequency as the  $n = 8$  amplitude but their minima are not necessarily at zero amplitude.

### 2.3 Toroidal asymmetry of the precursor

The observed toroidal asymmetry differs from the usually assumed toroidal symmetry of instabilities in tokamak plasmas. A toroidal envelope can be caused by spatial beating of two superposed modes or by a toroidal localized mode. Both mode structures have been modelled and the resulting spectra compared with the measurements. Since the measured

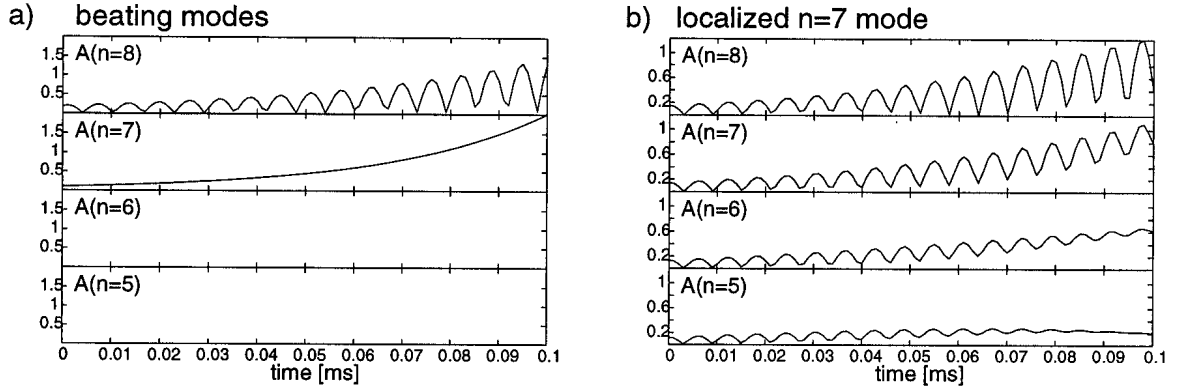


Figure 4: Modelled mode spectra of a) two growing beating modes  $n = 7$  and  $n = 8$  and b) a toroidally localized  $n = 7$  mode that grows in amplitude and toroidal extent measured with an array of 16 equally spaced probes and treated with the standard mode analysis. The mode spectrum of the toroidally localized  $n = 7$  mode shows the same characteristics as the measured mode spectrum in Fig. 3, in particular an oscillation of the amplitude of several mode components.

toroidal mode number is close to the resolution limit, the effects of discretization were studied by numerical simulations.

A superposition of two modes with  $\Delta n = 1$  and linear dispersion relation  $\omega_k = k\omega_0$ :

$$B(\phi_i, t) = \sum_{k=n', n'+1} A_k(t) \sin(k\phi_i - \omega_k t + \chi_{0k}) \quad (2)$$

shows a spatial beating that corresponds to a toroidal envelope of  $n = 1$  that rotates with  $\omega_0$ . The corresponding mode spectrum

$$A_n(t) = A_{n'}(t)\delta_{n',n} + A_{n'+1}(t)\delta_{n'+1,n} \quad (3)$$

is not as broad as the actual spectrum (Fig. 3) as it contains only two components. The magnetic signal of two simultaneous, exponentially growing modes with  $n = 7$ ,  $n = 8$  has been modelled for the TCV toroidal array and the calculated mode amplitudes are shown in Fig. 4a. Note that the  $n = 7$  component does not show the oscillating amplitude revealed in the experimental data (Fig. 3). Therefore, the model of beating modes does not describe all the characteristics of the observed mode spectra.

The observed spectrum can be explained by a toroidal localization of a perturbation with toroidal mode numbers close to  $n_{Ny}$ . Assuming a Gaussian toroidal weight of the

amplitude of the perturbation field

$$B(\phi_i, t) = A_{n'}^*(t) \cdot \exp[-\frac{1}{2}(\phi_i - \phi_{\max})^2 / \sigma_\phi(t)^2] \cdot \sin(n'\phi_i - \omega_{n'}t + \chi_{0n'}) \quad (4)$$

with an exponentially growing toroidal half width  $\sigma_\phi(t)$ , the expected mode spectra, for  $n, n' \gg \sigma_n$ , is approximately

$$A_n(t) \propto \exp[-\frac{1}{2}(n - n')^2 / \sigma_{n'}(t)^2]. \quad (5)$$

Since the half width of the spectrum  $\sigma_n$  depends inversely on the toroidal extend ( $\sigma_n = 1/\sigma_\phi$ ), a sufficiently localized mode results in a broad mode spectrum. The mode spectrum for a modelled localized mode (Eq. 4, Fig. 4b for  $n = 7$ ) shows the oscillating amplitude even for  $n \neq 8$ , as in the observed mode spectrum (see Fig. 3). Similar oscillations of the spectral amplitudes could be retrieved for localized  $n = 8$  and 9 modes.

## 2.4 Poloidal measurements

Measurements with a complete poloidal array, consisting of 38 equidistantly spaced probes, were performed on ELMy H-mode plasmas with a similar shape but with the plasma shifted towards the bottom of the vessel. The ELMs obtained during these discharges caused particle and energy losses typical for TCV large ELMs. They show coherent precursor oscillations with frequencies and growth rates similar to the described type III precursors. As for the toroidal measurements, the precursor could only be detected on the LFS of the plasma. Therefore, only a local poloidal mode number  $m_{\text{local}}$  which lies between 4 and 5 could be retrieved. Due to the highly elongated shape of the TCV vessel the poloidal spacing between adjacent probes on the equatorial midplane with respect to the magnetic axis was only  $24^\circ$ , resulting in a resolution limit of  $m_{\text{Ny}} = 7.5$ . Since the ELM is believed to be an edge phenomenon the expected poloidal mode number  $m = qn$  is masked by aliasing.

## 3 Summary and conclusion

In TCV magnetic oscillations are observed to precede ELMs believed to be type III ELMs, as well as TCV large ELMs. For both observed types of ELMs these precursors are



strongly localized on the LFS. They both show growth rates and frequencies, which are in the range of values found for type III precursors on ASDEX-Upgrade [4], which identifies TCV large ELMs also as large type III ELMs.

The precursor has a toroidally localized onset. The magnetic oscillation and particularly its mode spectrum is best described by a toroidally localized mode with a medium toroidal mode number  $n = 7 - 9$ . This mode grows in toroidal extent and amplitude while rotating in the electron diamagnetic drift direction. Following the toroidal extension, the encompassing of the entire toroidal circumference of the instability coincides with a broadening of the mode spectrum. At the same time the enhanced radial transport of particles and energy, corresponding to the rise of the  $D_\alpha$  signal, begins.

A medium toroidal mode number and a strong localization on the bad-curvature side support the hypothesis of a ballooning-like instability, as was first proposed for type III ELMs in ASDEX [5]. This has since been supported by observations on various experiments, and has formed the basis of theoretical approaches (see review articles [2, 6]).

Since the toroidally localized onset of the precursor differs from ELM to ELM and since the instability rotates toroidally, a localization due to errors in the measurements (i.e. hardware misalignment, gains) and a triggering of the ELM due to an asymmetry of the TCV assembly can be excluded. The asymmetry causing and supporting the precursor oscillation must be intrinsic to the plasma, possibly an underlying low- $n$  mode located in the high pressure gradient region close to the plasma edge. It has been shown that the stability of ideal ballooning modes is altered in the vicinity of a magnetic island [7]. The reduction of magnetic shear near the x-point of a magnetic island may destabilize a ballooning mode at one toroidal location [8]. Weak low  $n$  mode activity has been observed prior to ELMs in TCV, but a correlation between its phase and the onset of the precursor could not be retrieved. However, the rotation of the localized instability that precedes the ELM in the electron drift direction with typical values of low- $n$  mode rotation velocities and the observation of simultaneous onsets on opposite toroidal positions ( $n = 2$  symmetry) support this hypothesis.

## Acknowledgements

This work was partly funded by the Fond National Suisse de la Recherche Scientifique. The authors would like to acknowledge the help of J.-M. Moret, G. Tonetti and H. Weisen.

## References

- [1] WEISEN, H. et al., *Plasma Phys. Control. Fusion* **38** (1996) 1137.
- [2] ZOHM, H., *Plasma Phys. Control. Fusion* **38** (1996) 105.
- [3] BUTTERY, R. et al., in *Controlled Fusion and Plasma Physics (22nd Eur. Conf. Bournemouth, 1995)*, Vol. 19C, Part III, European Physical Society, Geneva (1995) 273.
- [4] KASS, T., et al., *Nucl. Fusion* **38** (1998) 111.
- [5] ASDEX Team, *Nucl. Fusion* **29** (1989) 1959.
- [6] CONNOR, J.W., A review of Models for ELMs, to appear in *Plasma Phys. Control. Fusion*.
- [7] HEGNA, C.C., CALLEN, J.D., *Phys. Fluids B* **4** (1992) 3031.
- [8] FREDRICKSON, E.D., et al., *Phys. Plasmas* **2** (1995) 4216.